Investigation of the Arbitrary Lagrangian Eulerian Formulation to Simulate Shock Tube Problems

C.P. Salisbury, D.S. Cronin, F.S. Lien
University of Waterloo

Abstract

A critical step in modeling complex problems using numerical simulations is validating the numerical approach using simplified problems. The current study investigates application of the Arbitrary Lagrangian Eulerian (ALE) formulation, as implemented in LS-DYNA, to simulate a pseudo 1-D shock tube problem. The shock tube problem was selected since analytical results can be directly determined from the initial conditions. A shock tube is modeled as two regions of fluid at two different pressures separated by a thin membrane. The two regions are usually, but not necessarily, comprised of the same fluid. One region, know as the driver, is at a higher pressure than the other. Ideally, the thin membrane is completely destroyed to initiate flow, allowing the high pressure region to interact with the low pressure region. If the difference in pressures between the two regions is sufficient, a shock wave will propagate into the low pressure region and an expansion wave will propagate into the high pressure region. The current study is conducted to test the ability of the ALE formulation in LS-DYNA to correctly predict the shock and expansion wave propagation seen in a shock tube test. The results of this study are dependent on a number of factors such as the size and orientation of the mesh. A convergence study to determine the minimum mesh density to correctly simulate the shock phenomena was also conducted. This is of special importance when the ALE formulation is used in real world problems where the required mesh size can become quite large, and therefore computationally prohibitive.

Introduction

A multitude of methods for numerically simulating compressible flow have been proposed in the past. However, many of these codes have been developed for specific fluid flow problems that, for the most part, do not allow for fluid-structure coupling. The ALE implementation in LS-DYNA allows for fluid-structure problems to be solved numerically.

The first critical step in performing a coupled analysis is to validate the numerical results using simplified problems. This is the topic of the current study. Analytical solutions for compressible flow behaviour have been developed for shock tube simulations. A shock tube contains two regions filled with gas at different pressures that are separated by a membrane. When the membrane is removed, the different pressures in the gas can create a shock wave. Additionally, an expansion wave and moving contact surface are created. These phenomena are of great importance when studying any type of compressible fluid flow behaviour.

Problem Formulation

A shock tube consists of two volumes separated by a membrane. Usually, one volume consists of a high pressure gas with the second volume consisting of a low pressure gas. The membrane is suddenly removed (either by electrical or mechanical means) exposing the high pressure gas to the area of low pressure. This creates a shock wave that propagates into the low pressure area and a rarefaction or expansion wave that propagates into the high pressure area. The type and temperatures of the gas can be different depending on the desired shock flow properties. Theoretical equations have been developed which allow calculation of all the flow properties, velocity, density, pressure and temperature, from the initial pressure ratio. Figure 1 is a schematic of the initial state and Figure 2 is at some time after the diaphragm has been ruptured.

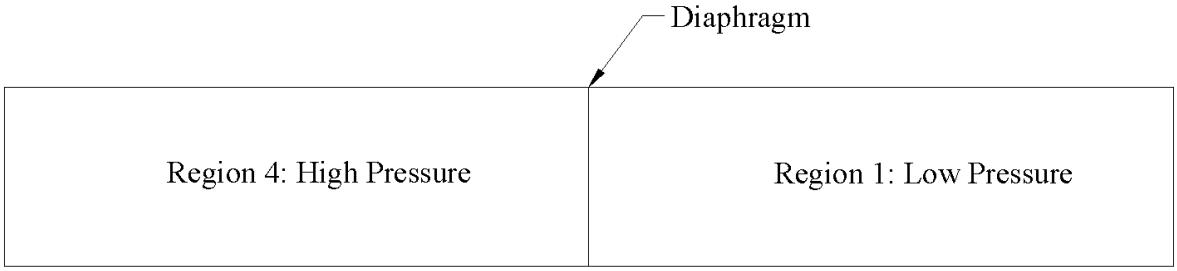

Figure 1: Initial Shock Tube Configuration

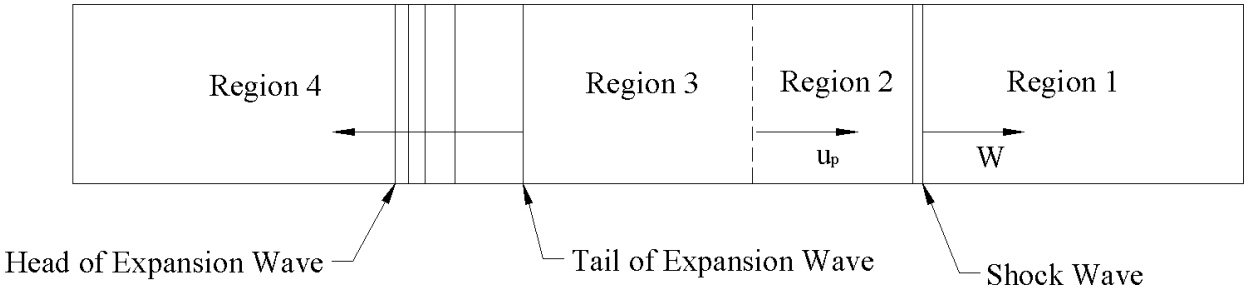

Figure 2: Waves in Shock Tube After Diaphragm Rupture

Figure 2 shows the various wave phenomena that occur in the shock tube. The rarefaction wave that occurs from region 3 to region 4 is continuous and follows an isentropic expansion. The expansion wave can be thought of as multiple Mach waves moving at different velocities. The method of characteristics [1] is used to solve for the velocity of the Mach waves between the head and tail of the expansion wave. This wave usually propagates to the left but can, depending on the initial conditions, propagate to the right. The dashed line between region 2 and region 3 represents the contact surface between the fluids initially in regions 1 and 4. This contact surface propagates to the right at a velocity of u_p. The pressure and velocity across the contact surface are continuous but the density and internal energy are not. The shock wave propagates to the right at a velocity W. Across the shock all properties are discontinuous.

A test case identified by LeVeque [2] uses a density and pressure ratio of 3 to test the ability of a calculation (code) to resolve compressible flow phenomena. This problem is similar to a scenario that would occur in a far field explosion event.

Analytical Solution

Analytical solutions to the shock tube problem can be determined from the conservation equations and the method of characteristics. From the initial conditions, p_2 / p_1 can be solved for by using the following relation:

$$\frac{p_4}{p_1} = \frac{p_2}{p_1}\left\{1 - \frac{(\gamma_4 - 1)(a_1 / a_4)(p_2 / p_1 - 1)}{\sqrt{2\gamma_1\left[2\gamma_1 + (\gamma_1 + 1)(p_2 / p_1 - 1)\right]}}\right\}^{-2\gamma_4/(\gamma_4 - 1)} \tag{1}$$

Once p_2 is solved for, the following relations apply:

$$p_2 = p_3 \tag{2}$$

$$\rho_2 \neq \rho_3 \tag{3}$$

$$u_2 = u_3 = u_p = u_c \tag{4}$$

$$\frac{p_3}{p_4} = \frac{p_3}{p_1}\frac{p_1}{p_4} = \frac{p_2}{p_1}\frac{p_1}{p_4} \tag{5}$$

$$\frac{p_3}{p_4} = \left(\frac{\rho_3}{\rho_4}\right)^{\gamma} = \left(\frac{T_3}{T_4}\right)^{\gamma/(\gamma-1)} \tag{6}$$

Using the conservation equations the shock speed can be calculated by:

$$W = a_1\sqrt{\frac{\gamma+1}{2\gamma}\left(\frac{p_2}{p_1} - 1\right) + 1} \tag{7}$$

The density across the shock is given by:

$$\frac{\rho_2}{\rho_1} = \frac{1 + \dfrac{\gamma+1}{\gamma-1}\dfrac{p_2}{p_1}}{\dfrac{\gamma+1}{\gamma-1} + \dfrac{p_2}{p_1}} \tag{8}$$

The following relations apply through the expansion fan:

$$u = \frac{2}{\gamma+1}\left(a_4 + \frac{x}{t}\right) \tag{9}$$

$$\frac{a}{a_4} = 1 - \frac{\gamma-1}{2}\left(\frac{u}{a_4}\right) \tag{10}$$

$$\frac{p}{p_4} = \left[1 - \frac{\gamma-1}{2}\left(\frac{u}{a_4}\right)\right]^{2\gamma/(\gamma-1)} \tag{11}$$

$$\frac{\rho}{\rho_4} = \left[1 - \frac{\gamma-1}{2}\left(\frac{u}{a_4}\right)\right]^{2/(\gamma-1)} \tag{12}$$

Numerical Implementation

Two key factors that affect shock resolution using the ALE formulation are mesh density and mesh orientation. Four models of different mesh densities (dx=0.0025, 0.005,0.01,0.02) at a 0^o orientation were created to explore the effects of mesh density. Two meshes of different densities (dx=0.006,0.012) at a 45^o orientation were created to explore orientation effects. Figures 3a and 3b show the mesh density at the 0^o orientation for the coarsest and finest cases. Figures 4a and 4b show the mesh for the coarse and fine cases with the 45^o mesh orientation.

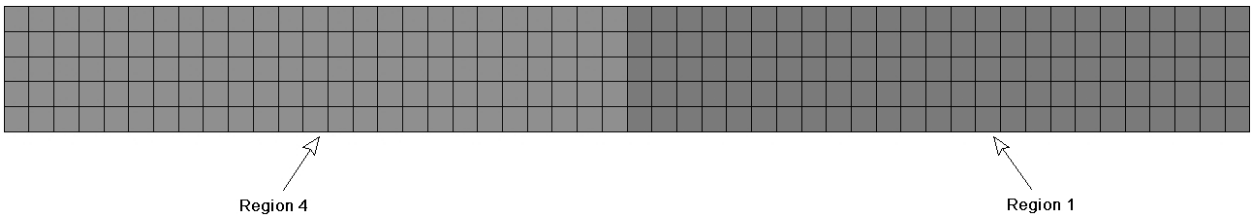

Figure 3a: Coarse Mesh dx=0.02

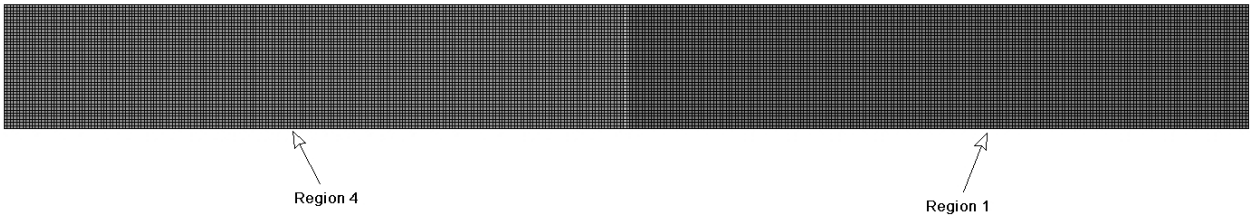

Figure 3b: Fine Mesh dx=0.0025

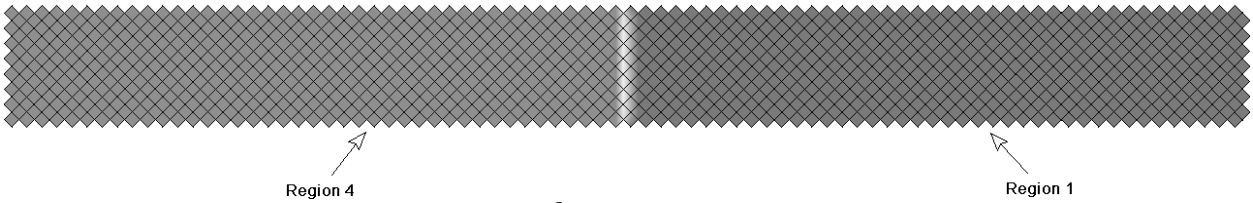

Figure 4a: 45^o Coarse Mesh dx=0.012

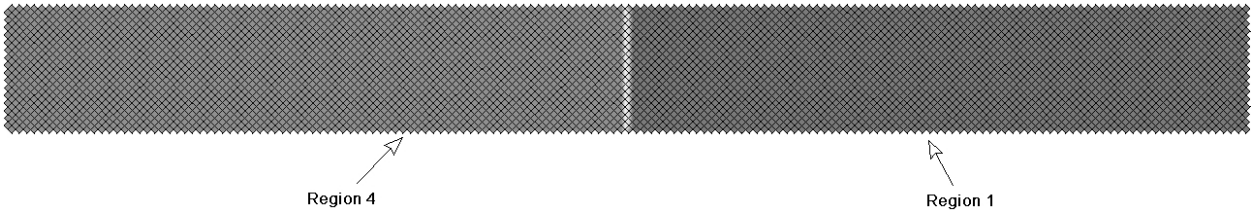

Figure 4b: 45^o Fine Mesh dx=0.006

The distance, dx, between the center of the elements are different between the 0^o and 45^o cases due to the orientation of the mesh. The mesh density was based on the element length, Δ. The relation between dx and Δ is shown in Figure 5.

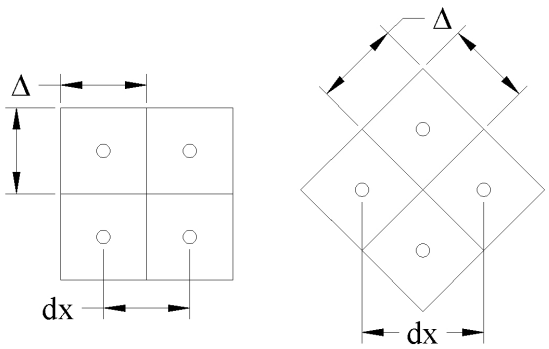

Figure 5: Mesh Orientation and Variable Spacing

Since the shock tube calculations are based on a one-dimensional problem, certain boundary conditions are assumed in the analytical solution, and must be represented in the numerical solution. Three dimensional, multi-material ALE, hexagonal elements were used in this problem. Three dimensions were reduced to two by using an element thickness (length of the element in the Z direction) of 0.01 and constraining all motion in Z direction, where the Z coordinate is through the thickness. Domain boundaries were created by constraining the motion of the nodes. Nodes on the top and bottom surfaces were constrained in the Y (vertical) direction with nodes on the left and right surfaces constrained in the X (horizontal) direction. This was done for both the 0^o and 45^o cases. By constraining the nodes, perfectly reflective surfaces were created. Therefore, analysis of the results was only valid until the waves were able to reflect off the left or right boundaries of the mesh. These results were compared to the analytical solution of the shock tube problem.

Results

Figure 6 shows contours of pressure for the finest 0^o mesh model at t=0.05s. Since Figure 6 only shows contours of pressure, the contact surface between regions 2 and 3 is not obvious. Figure 6 shows the expansion fan as a continuous gradient of pressure. The shock wave is identified by the discontinuous change in pressure.

Figure 7a compares results of the analytical and numerical solutions for the 0^o problem. Figures 7b and 7c show the solutions through the expansion fan and across the shock wave.

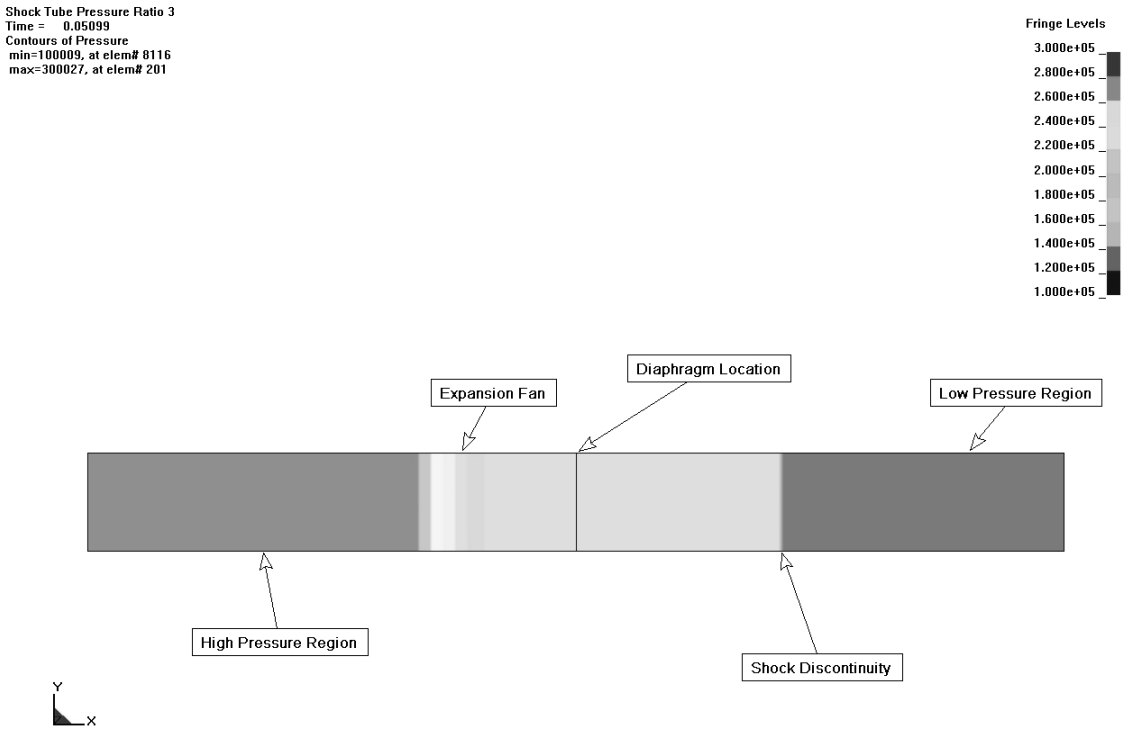

Figure 6: LS-DYNA Model Showing Shock Tube Waves, dx=0.0025, t=0.05s

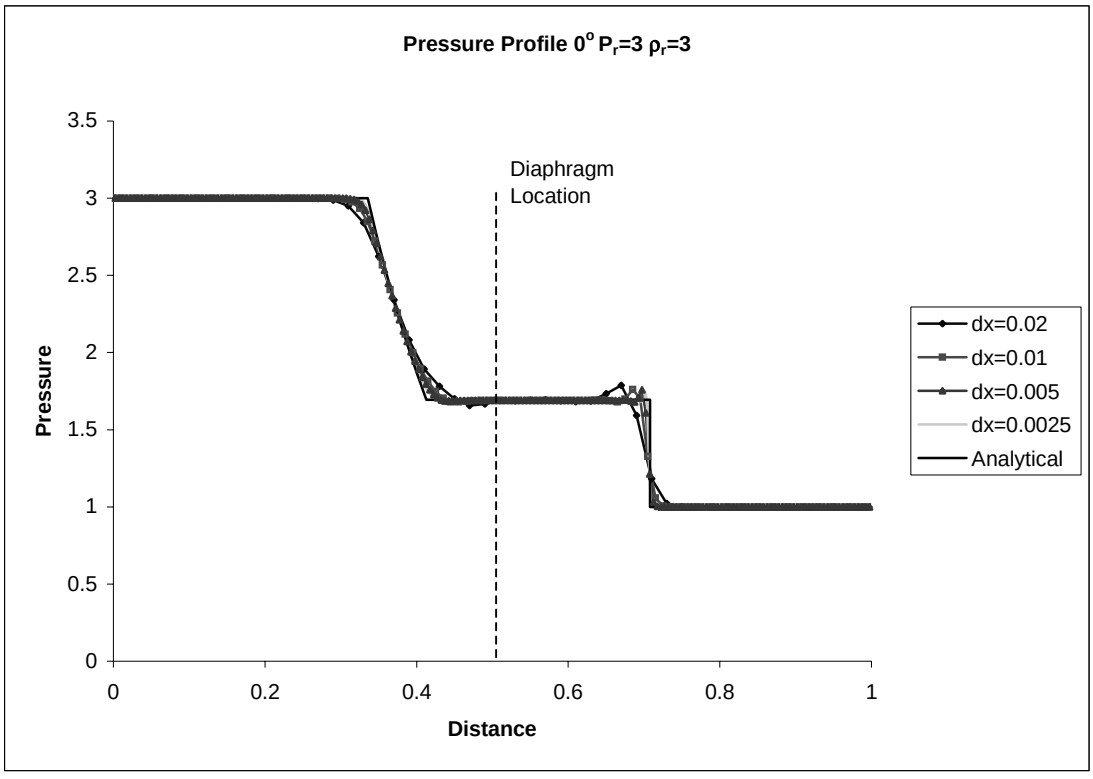

Figure 7a: Pressure Profile 0^o Mesh

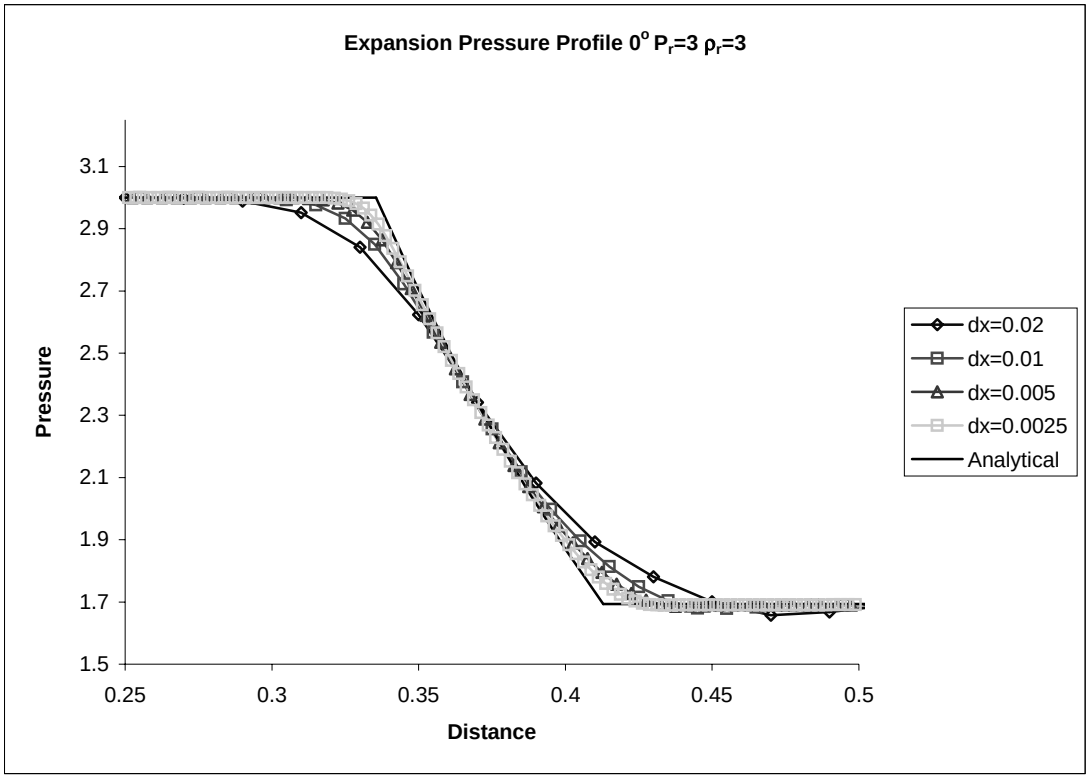

Figure 7b: Expansion Pressure Profile 0^o Mesh

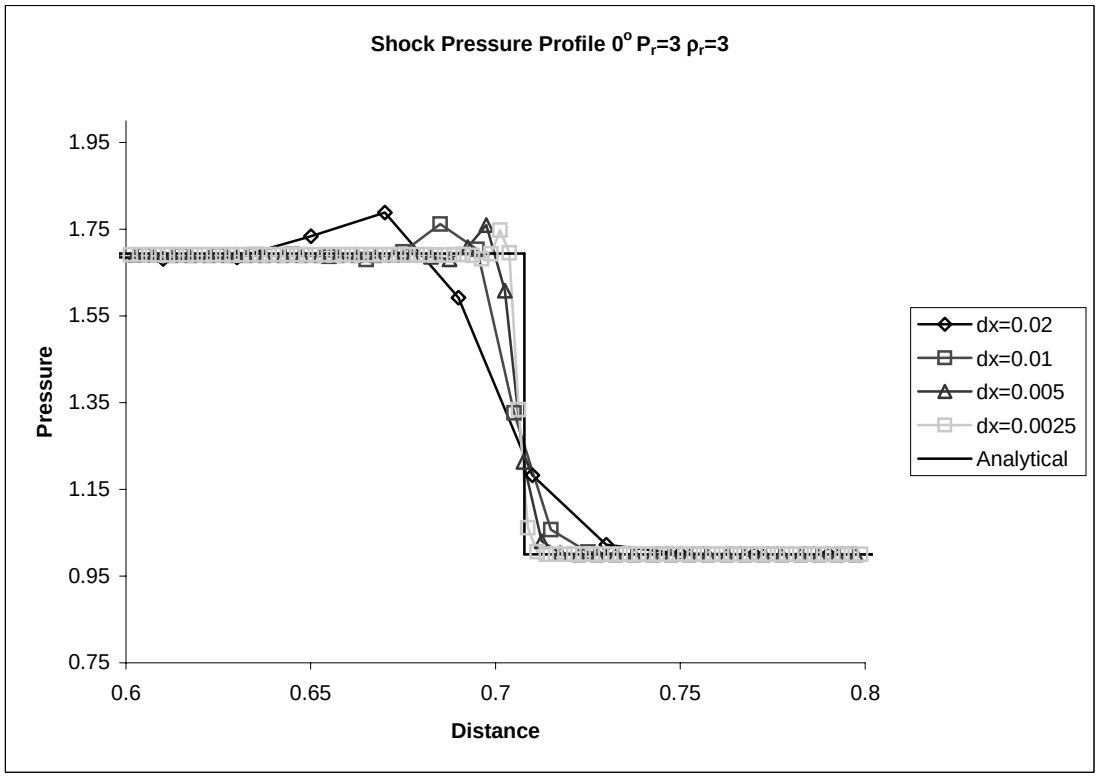

Figure 7c: Shock Pressure Profile 0^o Mesh

Figures 7a through 7c show a relatively good correlation for pressure between the analytical and numerical results. Only minor oscillations in region 2 and 3 are observed, and only for the

coarsest mesh in Figure 7a. Some undershoot is seen through the transition zone for the expansion fan in Figure 7b. Some overshoot is seen for the shock pressure profile in Figure 7c. For both the expansion and shock pressure profiles the numerical results approach the analytical results as mesh density increases. The difference between dx=0.005 and dx=0.0025 mesh is minimal indicating convergence.

Figures 8a through 8c show that the correlation between the numerical and analytical solution for the 45^o case is not as good as that for the 0^o mesh case. Some oscillations occur in pressure regions 2 and 3. Numerical interpretation of the expansion fan and shock discontinuity is also less accurate in this case. These discrepancies arise from the way in which the material is advected from one cell to another in the ALE algorithm.

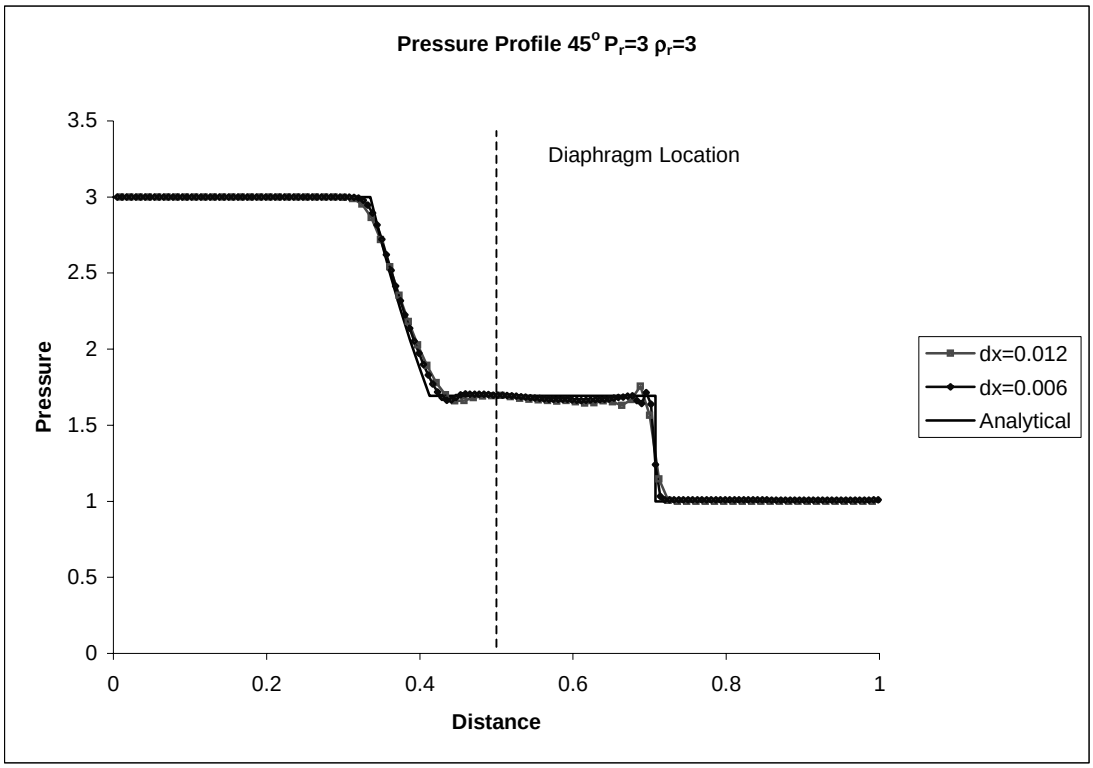

Figure 8a: Pressure Profile 45^o Mesh

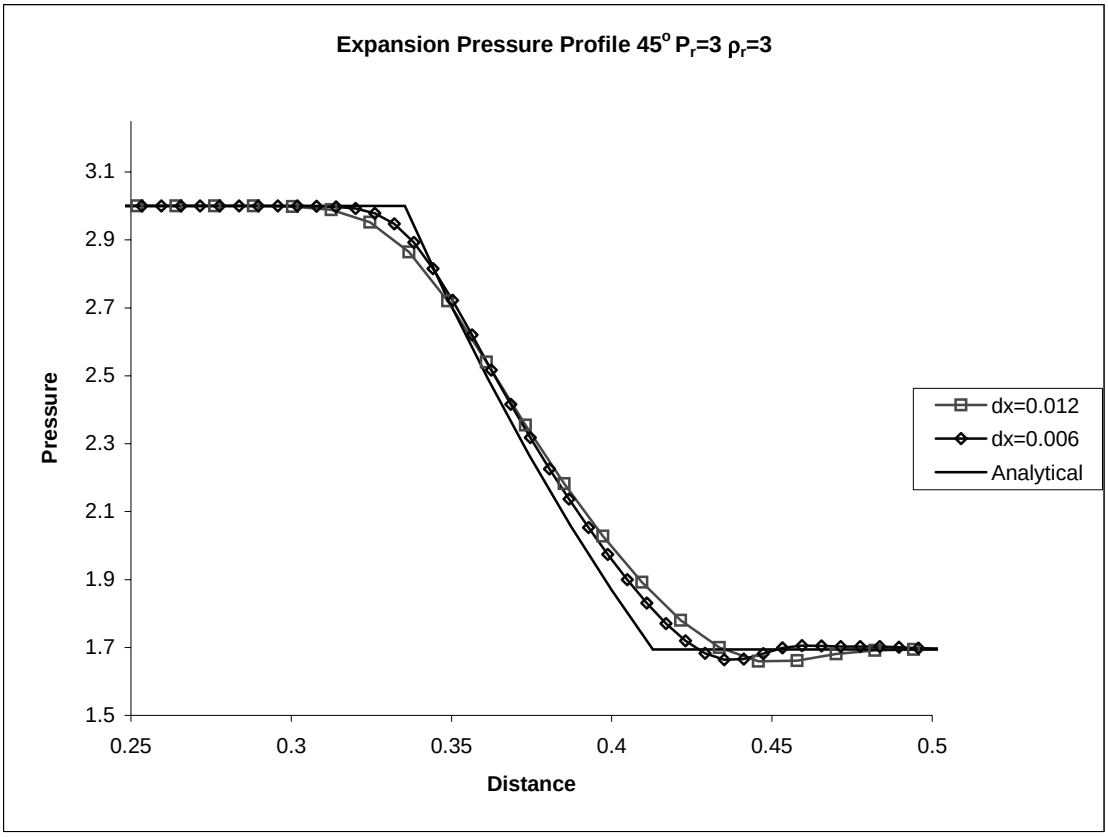

Figure 8b: Expansion Pressure Profile 45° Mesh

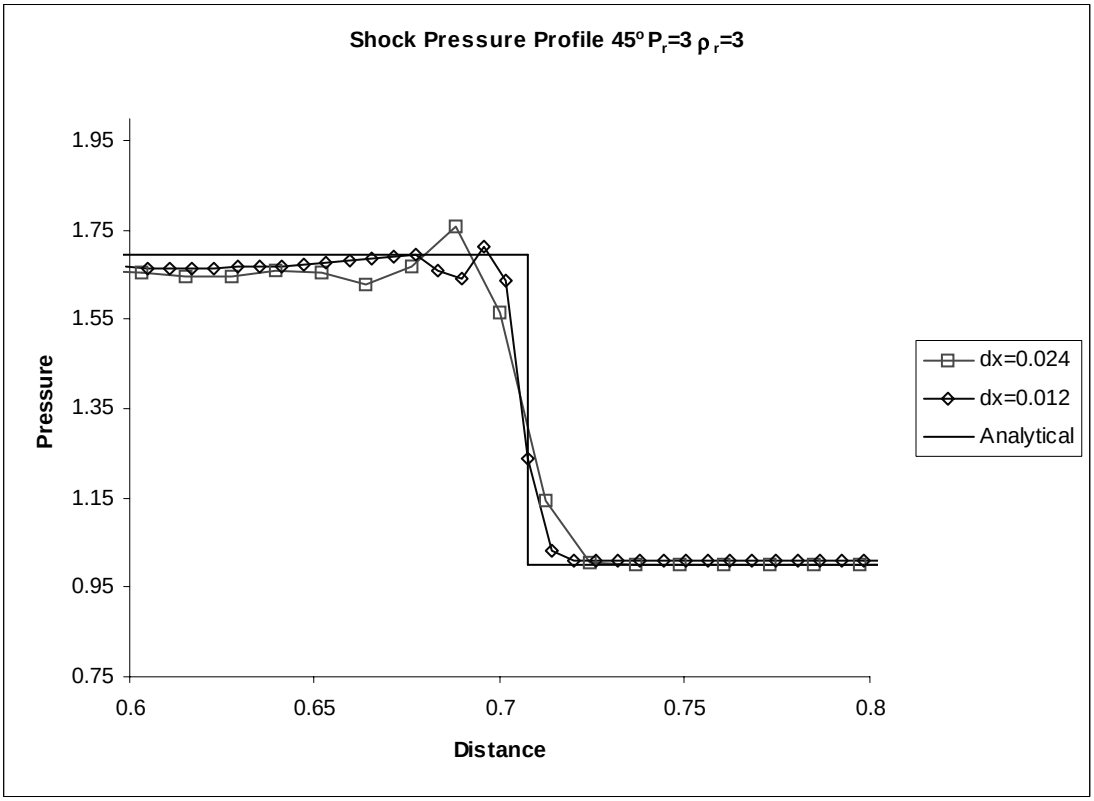

Figure 8c: Shock Pressure Profile 45° Mesh

Figures 9a and 9b show the density profile for the 0^o and 45^o meshes. Similar to the pressure profile, the density profile for the 0^o mesh shows a good correlation with the predicted values. The behaviour through the contact surface is similar to that of the shock discontinuity although less overshoot is seen. Increasing the mesh density increases the resolution of both the contact and shock discontinuity. Once again, increasing the mesh density from dx=0.005 to dx=0.0025 results in only a minor change in predicted density, showing convergence. The 45^o mesh exhibits similar behaviour as before. Of noticeable difference is the contact surface. The model fails to intersect the contact surface picking up only the beginning of the discontinuity. This is most likely due to the method through which the flow variables are advected. Figure 10 is a schematic indicating how flow variables are advected with the ALE algorithm. When the mesh is oriented perpendicular and parallel to the flow direction the fluid is able to advect directly across the element boundaries into the adjacent cell. When the mesh is 45^o to the flow direction, the flow variables are advected to the diagonally adjacent cells before being advected into the adjacent cell as indicated in Figure 10. This creates a two dimensional effect as indicated in Figure 11.

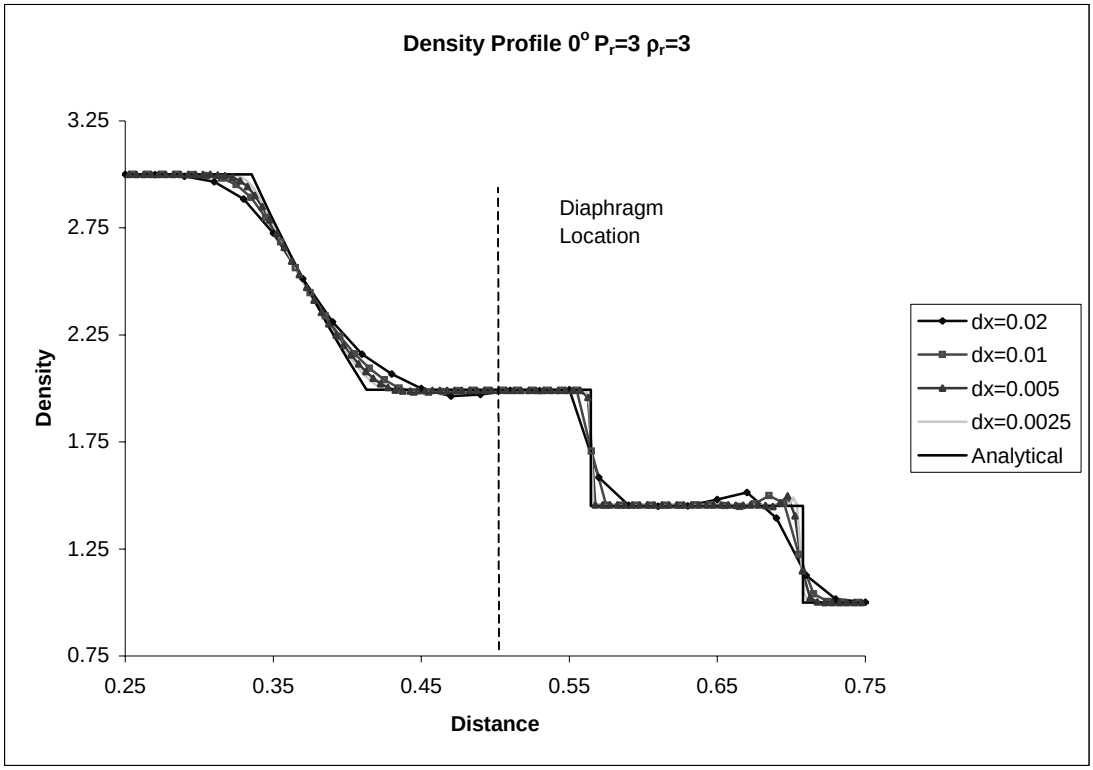

Figure 9a: Density Profile 0^o Mesh

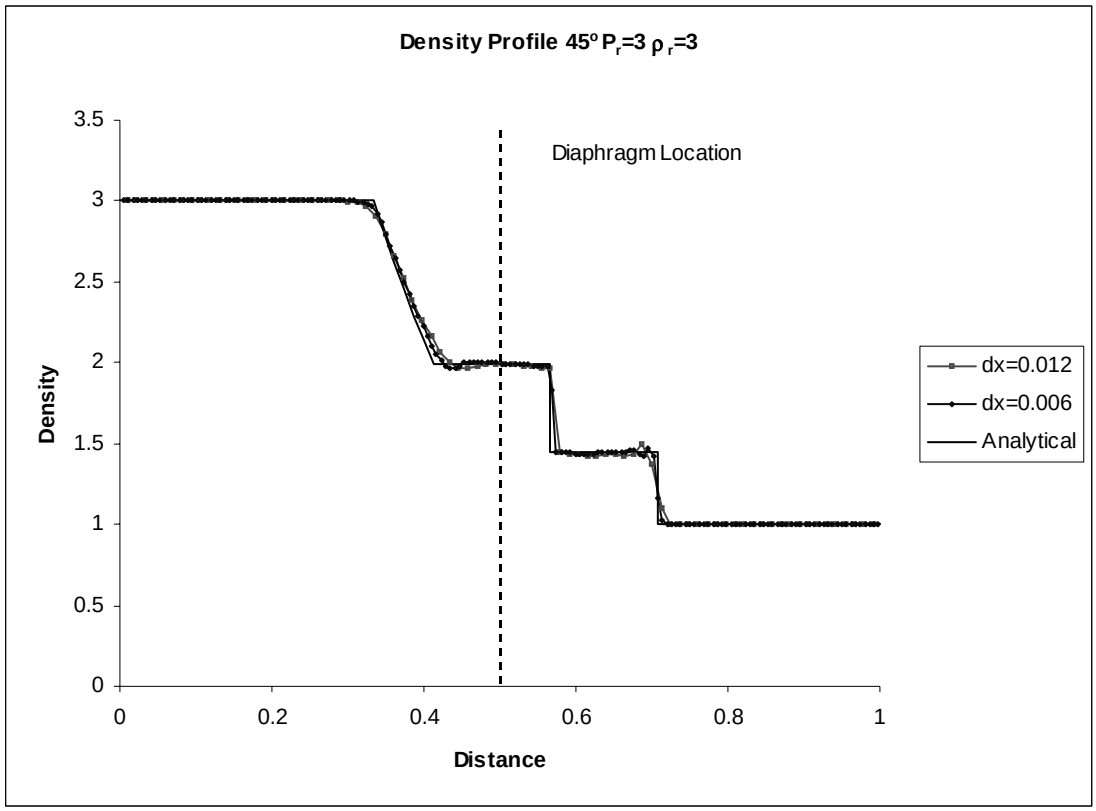

Figure 9b: Density Profile 45° Mesh

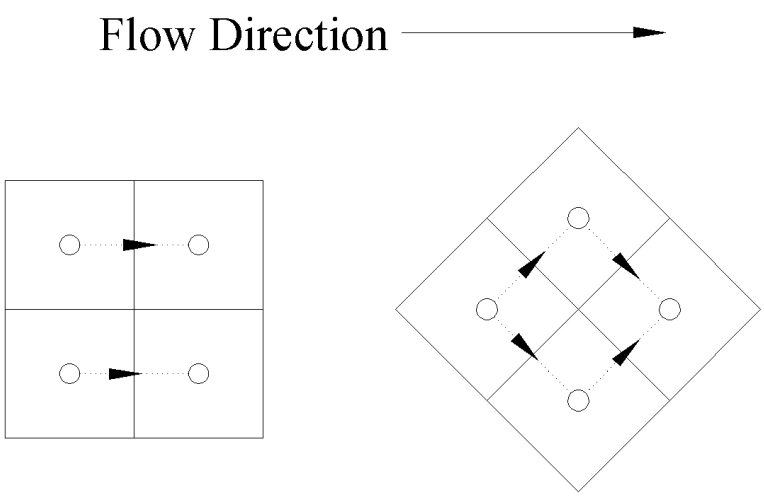

Figure 10: Advection Schematic

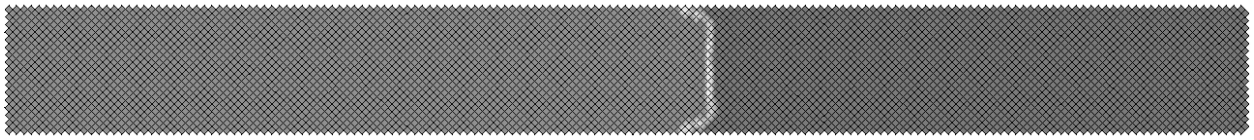

Figure 11: 2-Dimensional Effects for 45° mesh

Other test cases have also been considered. In an attempt to circumvent the possible boundary problems for the 45° case, a larger 45° mesh was created with a rigid shell that enclosed the

shock tube area to remove any boundary effects. The results from this analysis showed the effect in Figure 11, but to a greater extent. Additionally, the difference between the first order and second order advection methods was also explored. Only minor differences were apparent in these studies for the shock tube problem. Finally, a more extreme problem developed by Sod [3], which uses a pressure ratio of 10 and density ratio of 8 was also modeled. Some error was found in the time of arrival for the shock and expansion waves, but in general the results were in good agreement.

Conclusions

A convergence study was carried out to determine the ability of LS-DYNA to resolve shock fronts and expansion waves. A shock tube, for which an analytical solution exists, was used to compare to the numerical solutions. It was determined that the solution converged below and element size corresponding to dx=0.005. For most engineering problems, however, good approximation is possible with larger mesh sizes, reducing the computational cost. A similar mesh size but orientated at 45^o was also implemented to determine mesh orientation effects. Although less accurate than the 0^o mesh orientation, the numerical solution still correlated quite well with the exact solution. Increased, but tolerable oscillations and overshoots were seen.

In addition, there was good correlation based on material density as well, with accuracies similar to those shown for the 0^o pressure profile. The 45^o finite element mesh orientation displayed reduced accuracy, in particular at the contact interface.

References

[1] Anderson, J.D. Jr, 1990, *Modern Compressible Flow with Historical Perspective*, McGraw-Hill, Boston

[2] Leveque, R.J., *Numerical Methods for Conservation Laws*, Birkhauser Verlag, Berlin, Germany, 1992.

[3] Sod, G.A., "A Survey of Several Finite-Difference Methods for Systems of Nonlinear Hyperbolic Conservation Laws," Journal of Computational Physics, Volume 27 (1978), p. 1-31